Received: 25 April 2024 | Accepted: 18 July 2024

DOI: 10.1002/pamm.202400021

RESEARCH ARTICLE

Brittle fracture investigation in a coupled FEM-PD model

Anna Pernatii[1] | **Danylo Filiurskyi**[1] | **Ulrich Gabbert**[1] | **Jan-Timo Hesse**[2] | **Christian Willberg**[3]

[1]Institute of Mechanics, Otto-von-Guericke University Magdeburg, Magdeburg, Germany

[2]Institute of Composite Structures and Adaptive Systems, German Aerospace Center (DLR), Braunschweig, Germany

[3]Institute of Material Science, Magdeburg-Stendal University of Applied Science, Magdeburg, Germany

Correspondence
Anna Pernatii, Institute of Mechanics, Otto-von-Guericke University Magdeburg, Germany.
Email: anna.pernatii@ovgu.de

Funding information
Deutsche Forschungsgemeinschaft, Grant/Award Number: 456427423

Abstract

The simulation of crack patterns, crack velocities, and dissipated energies is a challenging task. Peridynamics (PD) has been proven to be a powerful tool addressing all these problems, including crack propagation, crack branching, its velocity and delamination, and so forth. It is a nonlocal theory, where material points interact with other points (these interactions are called bonds) within a continuous neighborhood in a specific range, called horizon. Typically, for complex problems PD is solved numerically. Its implementations require a high spatial resolution for adequate representation of the damaged material behavior, which is related to the high computational costs. Additionally, because of the nonlocal nature of PD there are difficulties in applying the classical local initial and boundary conditions. This leads to the idea of coupling relatively expensive PD with a finite element method to reduce the computational efforts and also try to solve the boundary condition problem. If the whole domain can be divided into two subdomains, the area where the fracture is expected should be modeled with the PD and the rest with finite elements. The present work proposes a comparison of three coupling strategies in terms of damage-free dynamic problems with high-frequency excitement. Additionally the investigation of the influence of wave propagation on the fracture process, as well as on crack patterns is presented.

1 | INTRODUCTION

The field of damage mechanics deals with understanding and predicting the fracture behavior of materials and structures under various loading conditions. It plays a crucial role in engineering, as it helps design safe and reliable structures, machines, and components. The main task is identifying potential failure mechanisms and understanding how damage initiates and propagates within a material or structure. Classical damage theory cannot predict crack initiation as well as crack branching phenomena, so many non-classical damage theories have been developed. Among them are: the cohesive zone model [1], the molecular dynamics [2], the phase-field methods [3], the damage gradient approach [4] and so forth. Nevertheless, the majority of theories often struggle to capture long-range effects and ignore the nonlocal character of damage processes, or they have a significant number of constitutive parameters that demand experimental identification.

Peridynamics (PD), on the contrary, is a nonlocal theory with an easy damage concept implemented in the governing equation. The internal forces are described by nonlocal interactions occurring between pairs of material points distributed throughout a continuous body. To take advances from the formulation, typically, it is implemented in a mesh-free form. In that case, separating interactions between different material points is easy. However, a relatively high resolution is required to describe continuous deformation functions. While PD demands less computational effort than some damage theories, which give similar accuracy regarding fracture, the processing time is still less efficient compared to classical computational methods. Besides, these classical approaches, such as the finite element method (FEM), can be categorized as local ones in the sense that a material point interacts just with its direct neighbors.

Consequently, a coupling of PD and FEM may have a great prospect in solving dynamic fracture problems also overcoming calculation inefficiency. If a general model has a localized zone where the damage is predicted or already exists, it can be modeled with PD, and the damage-free domain can be discretized with finite elements. Many approaches have been proposed for a couple of local and nonlocal domains. Among them are the Optimization-Based Method [5], the Schwarz coupling [6], the Arlequin method [7, 8], the Quasi nonlocal [9] procedures, force-based Morphing [10] and Blending [11] approaches, the Splice method [12] and many others. In the following paper, we analyze three coupling approaches (Schwarz, Arlequin, and Splice) regarding the possibility of transferring information from one domain to an another. After that, we investigate the influence of the coupling zone on brittle damage behavior.

2 | THEORETICAL BACKGROUND

2.1 | FEM

FEM is the most popular method to solve numerically partial differential equations. Convert the strong formulation of a mechanical problem into a weak one, we get:

$$-\int_{\Omega_{\mathrm{FE}}} \left[\rho\delta\mathbf{u}^T\ddot{\mathbf{u}} + \delta\boldsymbol{\varepsilon}^T\boldsymbol{\sigma}\right] \mathrm{d}\Omega + \int_{\Omega_{\mathrm{FE}}} \delta\mathbf{u}^T\mathbf{f}_V \,\mathrm{d}\Omega_+ \int_{\partial\Omega_{\mathrm{FE}}} \delta\mathbf{u}^T\mathbf{f}_{\partial\Omega}\,\mathrm{d}(\partial\Omega) + \sum_{i=1}^{n} \delta\mathbf{u}_i^T\mathbf{f}_i = 0\,, \tag{1}$$

with the mass density ρ, the displacement $\mathbf{u}$, the acceleration field $\ddot{\mathbf{u}}$, the stress tensor $\boldsymbol{\sigma}$, the strain tensor $\boldsymbol{\varepsilon}$, and $\mathbf{f}_\Omega$, $\mathbf{f}_{\partial\Omega}$, and $\mathbf{f}_i$ as volume, surface and nodal forces, respectively.

In the finite element approach, the entire body is divided into a finite number of elements and the displacement behavior on each element is predicted using shape functions: $\mathbf{u}(\mathbf{x}) = \mathbf{N}_u(\mathbf{x})\mathbf{u}_{\mathrm{N}}$. A similar approximation of the mechanical strain, using the derivatives of the shape functions results in: $\boldsymbol{\varepsilon}(\mathbf{x}) = \mathbf{B}_u(\mathbf{x})\mathbf{u}_{\mathrm{N}}$. If the approximation of the mechanical displacements equation and the strains equation is substituted in Equation (1) the equations are obtained as:

$$\delta\mathbf{u}_{\mathrm{N}}^T\int_{\Omega_{\mathrm{FE}}} \mathbf{N}_u^T\rho\mathbf{N}_u\mathrm{d}\Omega\,\ddot{\mathbf{u}}_{\mathrm{N}} + \delta\mathbf{u}_{\mathrm{N}}^T\int_{\Omega_{\mathrm{FE}}} \mathbf{B}_u^T\mathbf{C}^E\mathbf{B}_u^{\mathrm{dV}}\mathbf{u}_{\mathrm{N}}\mathrm{d}\Omega = \delta\mathbf{u}_{\mathrm{N}}^T\int_{\Omega_{\mathrm{FE}}} \mathbf{N}_u^T\mathbf{F}_\Omega\mathrm{d}\Omega + \delta\mathbf{u}_{\mathrm{N}}^T\int_{\partial\Omega_{\mathrm{FE}}} \mathbf{N}_u^T\mathbf{F}_{\partial\Omega}\mathrm{dS}(\partial\Omega) + \delta\mathbf{u}_{\mathrm{N}}^T\mathbf{N}_u^T\mathbf{F}_P. \tag{2}$$

The equation is valid for any variation $\delta\mathbf{u}$, so that it can be brought into the following form:

$$\mathbf{M}\ddot{\mathbf{u}}_{\mathrm{N}} + \mathbf{K}\mathbf{u}_{\mathrm{N}} = \mathbf{F}_{ext}. \tag{3}$$

with mass matrix $\mathbf{M}$, stiffness matrix $\mathbf{K}$ and external force vector $\mathbf{F}_{ext}$, each of them can be calculated for every element:

$$\mathbf{M} = \int_{\Omega_{\mathrm{FE}}} \mathbf{N}_u^T\mathbf{N}_u \,\mathrm{d}\Omega; \qquad \mathbf{K} = \int_{\Omega_{\mathrm{FE}}} \mathbf{B}_u^T\mathbf{C}\mathbf{B}_u \,\mathrm{d}\Omega;$$

2.2 | PD

In the current section bond-based PD is considered, that was presented by Silling [13]. Let two particle in a body are called as $\mathbf{x}$ and $\mathbf{x}'$, than the relative position of these two particles is called a bond $\boldsymbol{\xi} = \mathbf{x}' - \mathbf{x}$. Under the external load each

material point $\mathbf{x}$ in the body gets the displacement $\mathbf{d}$. The relative displacement can be found as $\boldsymbol{\eta} = \mathbf{d}' - \mathbf{d}$. The sum $\boldsymbol{\xi} + \boldsymbol{\eta}$ represents the current relative position. In bond-based PD the interaction between particles occurs not just with direct neighbors but with all particles inside the nonlocal neighborhood. The radius of this neighborhood is called horizon δ and defines the grad of non-locality. Let the material be microelastic, so that the pairwise force function has a form:

$$\mathbf{f}(\boldsymbol{\xi}, \boldsymbol{\eta}) = \frac{\partial \mathrm{w}(\boldsymbol{\xi}, \boldsymbol{\eta})}{\partial \boldsymbol{\eta}} = \frac{c(\boldsymbol{\xi}) s^2 |\boldsymbol{\xi}|}{2}, \tag{4}$$

where w is a micro-potential, that defines the energy in a single bond, c is the micro-modulus and s is the bond stretch:

$$s = \frac{|\boldsymbol{\xi} + \boldsymbol{\eta}| - |\boldsymbol{\xi}|}{\boldsymbol{\xi}}. \tag{5}$$

The general equation of motion than looks as follow:

$$\rho\, \ddot{\mathbf{d}}(\mathbf{x}, t) = \int_{\Omega_{\mathrm{PD}}} \mathbf{f}(\mathbf{d}' - \mathbf{d}, \mathbf{x}' - \mathbf{x}, t) \mu(\boldsymbol{\xi}, t) \mathrm{dV}_{\mathbf{x}'} + \mathbf{b}(\mathbf{x}, t), \tag{6}$$

where $\mu(\boldsymbol{\xi}, t)$ is a time dependent function, that shows whether the bond is broken. It can take on values of either 1, if the current bond stretch is smaller, than its critical value s_0, or 0, in any other cases. The critical stretch value s_0 can be derived from the consideration of the equality of the strain energy density in classical mechanics and PD theories, and it can be expressed as follows:

$$s_0 = \sqrt{\frac{5G_0}{9k\delta}}, \tag{7}$$

with G_0 as energy release rate and k as bulk modulus.

2.3 | Schwarz method

The Schwarz domain decomposition is one of the oldest domain decomposition methods. It was invented by Hermann Amandus Schwarz in 1869. Since then, various extensions and adaptations of this technique have emerged. In the paper at hand, our primary focus is on the Schwarz Alternating Method.

If the whole domain $\Omega \subset \mathbf{R}^1$ can be divided into two sub-domains: Ω_{FE} and Ω_{PD}, the intersection of these domains can be labeled as: $\Omega_o = \Omega_{\mathrm{FE}} \cap \Omega_{\mathrm{PD}}$. The advantage of the method is, that both regions communicate and exchange information just through the common boundaries. For the transition region only Dirichlet boundary conditions are considered, meaning that only the displacement is to be transferred from one subdomain to another. Define the interfaces $\Gamma_1 = \partial\Omega_{\mathrm{FE}} \cap \Omega_{\mathrm{PD}}$ and $\Gamma_2 = \partial\Omega_{\mathrm{PD}} \cap \Omega_{\mathrm{FE}}$, where $\partial\Omega$ stands for the external boundary of the corresponding region. The whole procedure is shown as follows:

- For the time step n set an initial displacement $\mathbf{u}^{\Gamma_1}$ on the boundary and solve for the whole Ω_{FE}: $\mathbf{M}\ddot{\mathbf{u}}^n(\mathbf{x}) + \mathbf{K}\mathbf{u}^n(\mathbf{x}) = \mathbf{F}^n, \quad \forall(\mathbf{x}) \in \Omega_{\mathrm{FE}}$.
- The condition for the region's transition: $\mathbf{u}^n(\mathbf{x}) \Rightarrow \mathbf{d}^n(\mathbf{x}), \quad \forall\, \mathbf{x} \in \Gamma_2$.
- (*) With obtained $\mathbf{d}^n$ on the boundary solve for Ω_{PD}: $\rho\ddot{\mathbf{d}}^n(\mathbf{x}) = \sum_{\mathrm{PD}} \mathbf{f}(\mathbf{d}', \mathbf{d}, \mathbf{x}', \mathbf{x}) \mu^n V_{\mathbf{x}'} + \mathbf{b}^n, \quad \forall\, \mathbf{x} \in \Omega_{\mathrm{PD}} \notin \Gamma_2$.
- Find the displacement value on Γ_1 and pass it to the another subdomain: $\mathbf{d}^n(\mathbf{x}) \Rightarrow \mathbf{u}^n(\mathbf{x}), \quad \forall\, \mathbf{x} \in \Gamma_1$.
- Again find the solution just for the domain Ω_{FE}.
- If the convergence is reached with the predefined parameter ε: $\mathbf{u}^n(\mathbf{x}) - \mathbf{d}^n(\mathbf{x}) \leq \varepsilon, \quad \forall\, \mathbf{x} \in \Gamma_1$, than go to the next time step $n = n + 1$, if not—go to the step (*).

2.4 | Splice

The coupling strategy is based on the idea of dividing the whole domain into two subdomains belonging to FEM and PD subregions, but there is no region where the nodes of both types are present. To formulate the mass and stiffness matrices, the following should apply: FEM nodes acting only on other FEM nodes, besides PD points can "see" FEM nodes and thus act on them. In other words, the FEM node is treated in the same way as in classical theory, but the PD node will create bonds to the FEM nodes, which are embedded in its horizon, thus creating non-diagonal stiffness values in the global stiffness matrix. The transition region is represented by elements, half of which are FEM nodes and half of which are PD nodes. For the sake of simplicity, the uniform grid spacing is used, meaning that for each FEM node, there is a corresponding PD node with the same grid spacing. Consequently, the global stiffness matrix is non-symmetric since the number of non-diagonal terms for PD nodes is greater than for FEM nodes.

To formulate the mass matrix, the same amount of mass is allocated to the FEM and PD nodes to ensure mass consistency, but it does not fully match the calculation of the PD node mass from theory. During the simulations, it was found that this particular issue did not affect the results, but it is still a valid point of discussion for us. The reader is referred to ref. [12] and also to the works of ref. [14] and ref. [15], where this coupling procedure is described in more detail.

2.5 | Arlequin method

The Arlequin Method is an energy-based coupling approach that allows a smooth transition between two sub-domains by weighting the model properties and characteristics through the overlap area [8]. The details of Arlequin coupling FEM-PD can be found in ref. [7] as the Lagrange-based approach and in ref. [16] as the Penalty-based one. Let the total Hamiltonian be written as below:

$$\mathbb{H}(\mathbf{u}, \dot{\mathbf{u}}, \mathbf{d}, \dot{\mathbf{u}}) = \alpha(\mathbf{x})\mathbb{H}_{\mathrm{FE}}(\mathbf{u}, \dot{\mathbf{u}}) + (1 - \alpha(\mathbf{x}))\mathbb{H}_{\mathrm{PD}}(\mathbf{d}, \dot{\mathbf{d}}), \tag{8}$$

with the weighting function $\alpha(\mathbf{x})$, that satisfy the following conditions:

$$\alpha(\mathbf{x}) = \begin{cases} & \forall \mathbf{x} \in \Omega_{\mathrm{FE}} \cap \Omega_o, \\ & \forall \mathbf{x} \in \Omega_{\mathrm{PD}} \cap \Omega_o, \\ \alpha(\mathbf{x}_0) & \forall \mathbf{x} \in \Omega_o. \end{cases} \tag{9}$$

The sum of energies in both theories is written as follows:

$$\mathbb{H} = \mathcal{W}^{kin} + \mathcal{W}^{int} - \mathcal{W}^{ext}, \tag{10}$$

The equation of motion is derived by taking the derivative of equation (10) by the displacement. Moreover, the additional constraints in the overlapping zone should be included. These constraints can be included using the Penalty Method. For this purpose, the functional Ψ should be constructed and demanded to reach a minimum value [17].

$$\Psi = \mathcal{L}(\mathbf{x}, \mathbf{u}, t) + \frac{1}{2}\kappa \int_{\Omega_o} \mathbf{z}^T \mathbf{z} d\,\Omega_o \rightarrow \mathrm{Min}, \tag{11}$$

where $\mathcal{L}$ is Lagrangian of the dynamic system, $\mathbf{z} = \mathbf{z}_0 + \mathbf{Z}\mathbf{u}$ are the constrains in a general form and κ is the penalty number. By minimizing the functional, the coupling terms with constrains are taking the form:

$$\mathbf{K}_z = \kappa \mathbf{Z}^T \mathbf{Z}; \qquad \mathbf{f}_z = \kappa \mathbf{Z}^T \mathbf{z}_0. \tag{12}$$

Thus, the equation of motion of the coupled system in discretized form looks as follows:

$$\begin{bmatrix} \frac{\alpha}{V_{\mathrm{el}}}\mathbf{M}_{\mathrm{FE}} & \\ & (1-\alpha)\rho_{\mathrm{PD}} \end{bmatrix} \begin{bmatrix} \ddot{\mathbf{u}} \\ \ddot{\mathbf{d}} \end{bmatrix} + \begin{bmatrix} \frac{\alpha}{V_{\mathrm{el}}}\mathbf{K}_{\mathrm{FE}} & \\ & (1-\alpha)\mathbf{f}_{\mathrm{PD}} \end{bmatrix} \begin{bmatrix} \mathbf{u} \\ \mathbf{d} \end{bmatrix} + \mathbf{K}_z \begin{bmatrix} \mathbf{d}^o \\ \mathbf{u}^o \end{bmatrix} = \begin{bmatrix} \frac{\alpha}{V_{\mathrm{el}}}\mathbf{F}_{\mathrm{FE}} \\ (1-\alpha)\mathbf{b}_{\mathrm{PD}} \end{bmatrix} \tag{13}$$

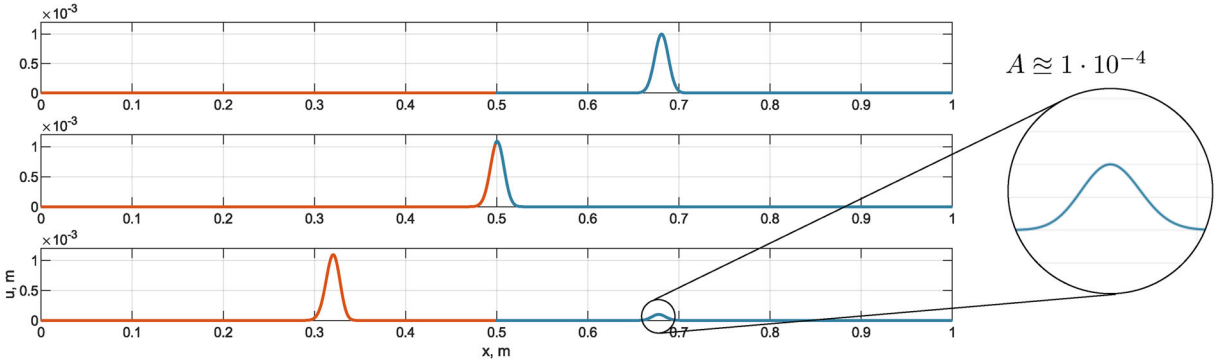

FIGURE 1 Wave propagation in a 1D bar, solved by the Schwarz coupling method at $t = 10^{-3}$ s, $t = 1.5 \cdot 10^{-3}$ and $t = 2 \cdot 10^{-3}$ s.

Here V_{el} is a volume of the current finite element. Some terms of the system here should be divided by V_{el} to match the dimensions between the theories.

3 | RESULTS AND DISCUSSION

3.1 | Wave propagation on 1D bar

To begin with, let us consider the 1D case: a bar of length 1 m is fixed on the left side. The Gaussian-type displacement function is applied on the right side: $\hat{u} = a\, e^{-\frac{(t-\beta)^2}{2c^2}}$, with the selected constants $a = 10^{-5}$ m, $\beta = 10^{-4}$ s, and $c = 210^{-6}$s. The material is assumed to be isotropic and elastic with parameters: $E = 10^9$Pa, $\nu = 0.25$, $\rho = 7800$ kg/m^2. The bar is divided into two pieces at the center, and every part is discretized either with finite elements or PD points with grid spacing (except for Schwarz coupling): $\Delta x_{\text{FE}} = \Delta x_{\text{PD}} = 5.5 \cdot 10^{-4}$ m. The other numerical parameter are $\delta = 3.015\,\Delta x$, $\Delta t = 1.5 \cdot 10^{-7}$ s and $t_{\text{tot}} = 2 \cdot 10^{-3}$ s.

First, the dynamic test is solved using the Schwarz Method. For this purpose, the mesh density parameter is proposed to stabilize the couple solution: $\text{md} = \frac{\Delta x_{\text{PD}}}{\Delta x_{\text{FE}}} = 25$, consequently one finite element and 25 PD points are used in the overlapping area. The results from Figure 1 give the wave propagation information on $t = 10^{-3}$ s, $t = 1.5 \cdot 10^{-3}$, and $t = 2 \cdot 10^{-3}$ s. It is to notice that a reflected wave with an amplitude $A \approx 1 \cdot 10^{-4}$ m and also a magnitude jump of the main wave occurs after it has passed the coupling region.

The Splice method shows a smooth transition of the displacement wave through the coupled region (Figure 3). Here, the uniform mesh is chosen for both domains, and no additional coupling parameters are considered. No noise is noticed by the naked eye. However, a small reflected wave with magnitude $A \approx 6 \cdot 10^{-7}$ m can be detected by the fast Fourier transform (FFT) method. The approach works quite well for wave propagation tests.

For the solution with the Arlequin method, the penalty parameter κ with the value 10^7 Pa/m is found as optimal and the cubic α-function was chosen. The bar is discretized with uniform constant mesh, and one overlapping FE and PD point is used. The results in Figure 2 show again the reflected wave on the last time step. However, the method gives more accuracy in comparison to the Schwarz approach.

To summarize, the Splice method gave the most accurate results. Using the Arlequin approach, a quite noticeable secondary wave appeared. However, the Schwarz algorithm responded with numerical errors and gave the worst solution in comparison to the previous methods. Altogether, even in the simplest 1D cases of coupling FEM and PD, the secondary wave is detected by high-velocity problems. Hence, it cannot be avoided entirely, though it is necessary to examine whether it influences the damage behavior of the system.

3.2 | Damage behavior in 2D plate

The rectangular plate 0.3×0.8 m^2 has an initial diagonal crack in the center. On the top and bottom edges, displacement is prescribed as a linear increasing function, dependent on time: $\bar{u} = 0.009\,\Delta t$. FEM zones are equal rectangles 0.3×1.5 m^2,

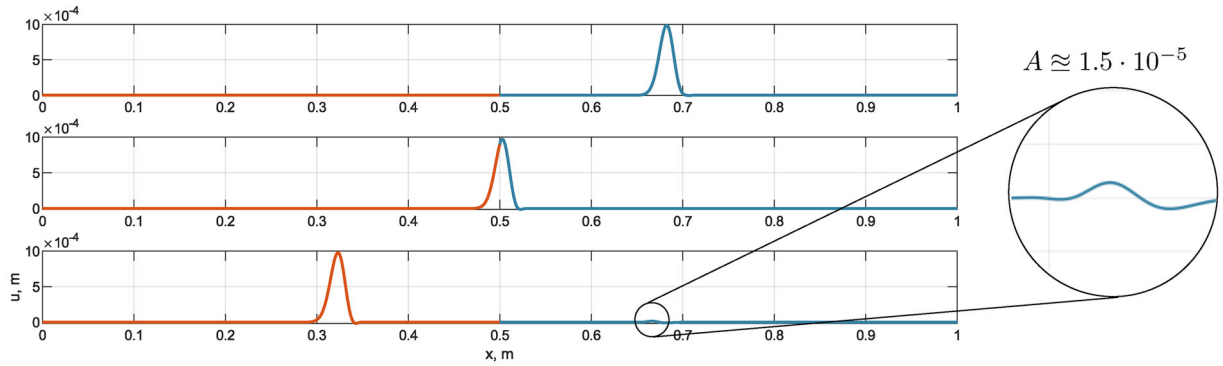

FIGURE 2 Wave propagation in a 1D bar, solved by the Arlequin coupling method at $t = 10^{-3}$ s, $t = 1.5 \cdot 10^{-3}$ and $t = 2 \cdot 10^{-3}$ s.

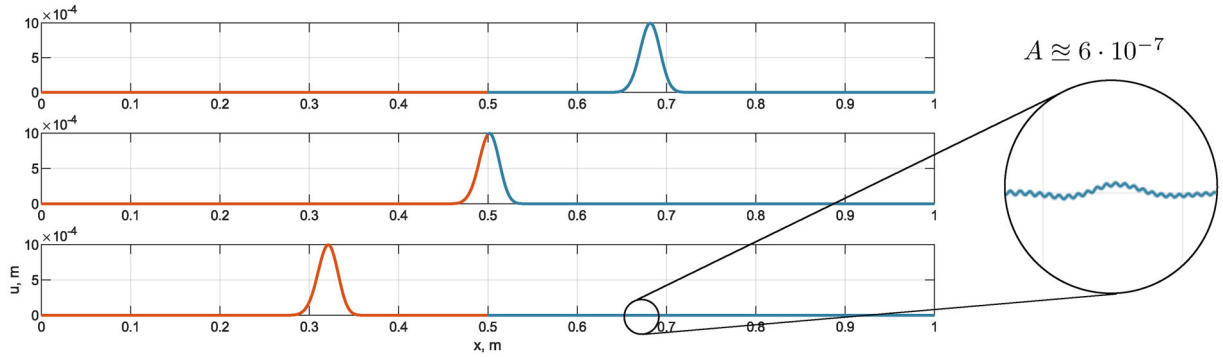

FIGURE 3 Wave propagation in a 1D bar, solved by the Splice coupling method at $t = 10^{-3}$ s, $t = 1.5 \cdot 10^{-3}$ and $t = 2 \cdot 10^{-3}$ s.

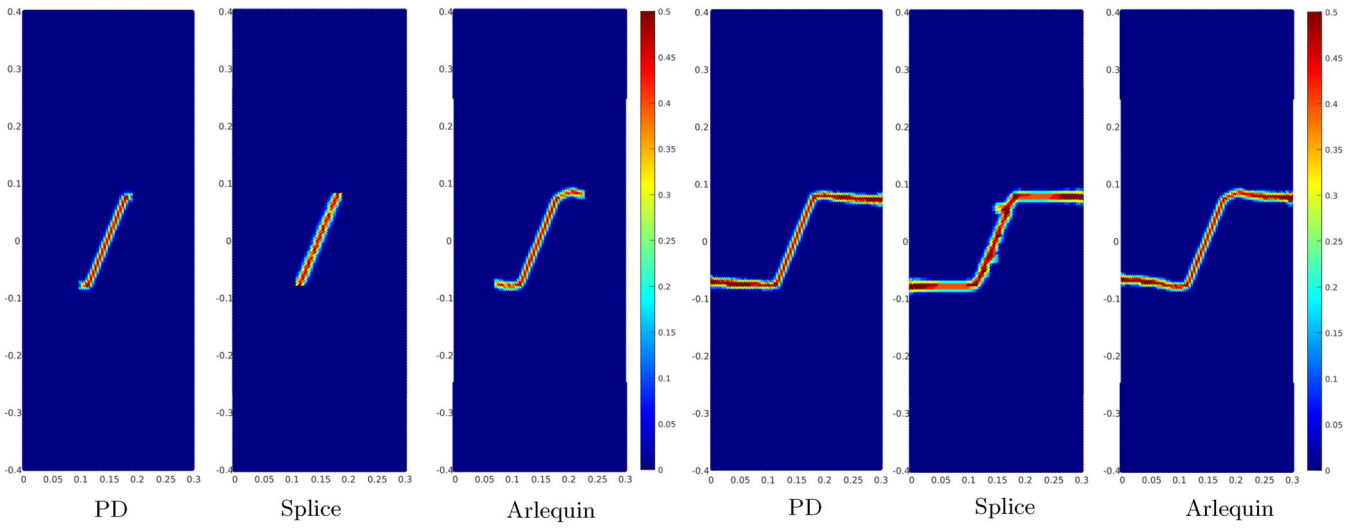

FIGURE 4 Fracture behavior in a 2D plate with diagonal initial crack at $t = 5.85 \cdot 10^{-5}$ s and $t = 6.8 \cdot 10^{-4}$ s.

located on the top and bottom of the plate. The remaining area is a PD domain. The material constants are taken from the previous tests, except $\nu = 0.33$, the energy release rate $G_0 = 3.8\,\mathrm{J/m^2}$, The numerical parameters are: $\kappa = E \cdot 10^4$ Pa/m, $\Delta t = 2.5 \cdot 10^{-7}$ s, $t_{\mathrm{tot}} = 6.8 \cdot 10^{-4}$ s, $\Delta x_{\mathrm{FE}} = \Delta x_{\mathrm{PD}} = 0.004$ m. As a reference solution the pure PD case is used. The damage picture for both three cases on time $t = 5.85 \cdot 10^{-5}$s are displayed on Figure 4. The crack starts to grow from both crack tips in a pure PD test, while in the Splice case, the crack does not move at this time. As we can notice, in Arlequin's

case, the crack has started to propagate earlier; the time difference is $\approxeq 2 \cdot 10^{-5}$ s. The last three plots illustrate the crack pattern in the last time step. Unexpectedly, the initial crack started to bifurcate, and a few small cracks appeared in the Splice case. On the contrary, the Arlequin result does not have such numerical artifacts and is in good agreement with a reference solution.

4 | CONCLUSION AND OUTLOOK

The article presents three FEM-PD coupling approaches; among them are the Schwarz, the Arlequin, and the Splice methods. These routines were implemented, and the behavior under high-velocity dynamic load was tested. Even though the Splice gave the most accurate result in 1D analysis, the extension to 2D depicts the problems to simulate precisely a damage behavior. A detailed analysis of the reasons and guidelines for improvement is a topic for future work. The Arlequin method is a promising approach that gave relatively good results regarding the crack patterns. The different loading cases, as well as the investigation of the influence of distance between the FEM domain and the damage zone in the PD area, will be shown in detail in future research.

ACKNOWLEDGMENTS

The project is funded by the Deutsche Forschungsgemeinschaft (DFG, German Research Foundation) under the Project number 456427423. This financial support is gratefully acknowledged.

Open access funding enabled and organized by Projekt DEAL.

ORCID

Anna Pernatii https://orcid.org/0000-0002-0004-0577
Jan-Timo Hesse https://orcid.org/0000-0002-3006-1520

REFERENCES

1. Zhou, F., Molinari, J. F., & Shioya, T. (2005). A rate-dependent cohesive model for simulating dynamic crack propagation in brittle materials. *Engineering Fracture Mechanics*, *72*(9), 1383–1410.
2. Abraham, F., Brodbeck, D., Rudge, W., & Xiaopeng, X. (1997). A molecular dynamics investigation of rapid fracture mechanics. *Journal of the Mechanics and Physics of Solids*, *45*(9), 1595–1619.
3. Boettinger, W. J., Warren, J. A., Beckermann, C., & Karma, A. (2002). Phase-field simulation of solidification. *Annual Review of Materials Research*, *32*(1), 163–194.
4. Lorentz, E., & Andrieux, S. (2003). Analysis of non-local models through energetic formulations. *International Journal of Solids and Structures*, *40*(12), 2905–2936.
5. Littlewood, D. J., Trageser, J., & Marta, D. (2021). An optimization-based strategy for peridynamic-FEM coupling and for the prescription of nonlocal boundary conditions. arXiv, 2110.04420.
6. Yu, Y., Bargos, F. F., You, H., Parks, M. L., Bittencourt, M. L., & Karniadakis, G. E. (2018). A partitioned coupling framework for peridynamics and classical theory: Analysis and simulations. *Computer Methods in Applied Mechanics and Engineering*, *340*, 905–931.
7. Wang, X., Kulkarni, S. S., & Tabarraei, A. (2019). Concurrent coupling of peridynamics and classical elasticity for elastodynamic problems. *Computer Methods in Applied Mechanics and Engineering*, *344*, 251–275.
8. Dhia, H. B., & Rateau, G. (1998). The Arlequin method as a flexible engineering design tool. *International Journal for Numerical Methods in Engineering*, *62*(11), 1442–1462.
9. Du, Q., Li, X. H., Lu, J., & Tian, X. (2018). A quasi-nonlocal coupling method for nonlocal and local diffusion models. *SIAM Journal on Numerical Analysis*, *56*(3), 1386–1404.
10. Lubineau, G., Azdoud, Y., Han, F., Rey, C., & Askari, A. (2012). A morphing strategy to couple non-local to local continuum mechanics. *Journal of the Mechanics and Physics of Solids*, *60*(6), 1088–1102.
11. Seleson, P., Ha, Y. D., & Beneddine, S. (2015). Concurrent coupling of bond-based peridynamics and the navier equation of classical elasticity by blending. *Journal of Multiscale Computational Engineering*, *13*(2), 91–113.
12. Galvanetto, U., Mudric, T., Shojaei, A., & Zaccariotto, M. (2016). An effective way to couple FEM meshes and peridynamics grids for the solution of static equilibrium problems. *Mechanics Research Communications*, *76*, 41–47.
13. Silling, S. A., & Askari, E. (2005). A meshfree method based on the peridynamic model of solid mechanics. *Computers & Structures*, *83*(17–18), 1526–1535.
14. Zaccariotto, M., Mudric, T., Tomasi, D., Shojaei, A., & Galvanetto, U. (2018). Coupling of FEM meshes with peridynamic grids. *Computer Methods in Applied Mechanics and Engineering*, *330*, 471–497.
15. Ongaro, G., Seleson, P., Galvanetto, U., Ni, T., & Zaccariotto, M. (2021). Overall equilibrium in the coupling of peridynamics and classical continuum mechanics. *Computer Methods in Applied Mechanics and Engineering*, *381*, 113515.

16. Pernatii, A., Gabbert, U., Naumenko, K., Hesse, J. T., & Willberg, C. (2023). A penalty method for coupling of finite–element and peridynamic models. *PAMM*, *22*(1), e202200151.
17. Gabbert, U. (1982). Berücksichtigung von zwangsbedingungen in der FEM mittels der penalty-funktion-methode. *Technische Mechanik*, *4*(2), 40–46.

How to cite this article: Pernatii, A., Filiurskyi, D., Gabbert, U., Hesse, J.-T., & Willberg, C. (2024). Brittle fracture investigation in a coupled FEM-PD model. *Proceedings in Applied Mathematics and Mechanics*, e202400021. https://doi.org/10.1002/pamm.202400021